A High-Performance and Robust Light Curve Inversion Method for Attitude Monitoring of Three-Axis Stabilised Satellites

Jorge Rubio[1,2], Adrián de Andrés[1]

[1]GMV, C. Isaac Newton 11, 28670, Tres Cantos, Madrid, Spain, jorge.rubio.anton@gmv.com, adandres@gmv.com

[2]Universidad Carlos III de Madrid, Av. de la Universidad 30, 28911, Leganés, Madrid, Spain, jorge.r.anton@alumnos.uc3m.es

Carlos Paulete[1], Ángel Gallego[1], José Miguel Lozano[2], Diego Escobar[1], Alberto Águeda[1]

[1]GMV, C. Isaac Newton 11, 28670, Tres Cantos, Madrid, Spain, cpauleteperianez@gmv.com, agtorrego@gmv.com, descobar@gmv.com, aagueda@gmv.com

[2]GMV, 2400 Research Blvd., Ste. 390, Rockville, MD 20850, USA, jmlozano@gmv.com

ABSTRACT

Accurate knowledge of the attitude of Resident Space Objects (RSOs) has become essential for different space debris mitigation activities, including collision risk assessment and atmospheric re-entry prediction. Attitude monitoring is also highly relevant in routine space operations for the detection of potential anomalies in controlled satellites. This study focuses on monitoring the attitude of three-axis stabilised satellites with known geometries using light curves. The worst-case scenario is considered, in which no prior knowledge of the attitude is available, thereby providing a realistic representation of operational conditions in which a satellite has deviated from its nominal attitude control mode. Moreover, the optical properties of the materials constituting the satellite's surfaces are assumed to be unknown, as their diversity makes them difficult to estimate. Even if the materials were well characterised, prolonged exposure to the space environment would likely cause ageing effects that unpredictably alter their optical properties.

In addition to the unknown optical properties, the proposed methodology is robust to uncertainties in Aerosol Optical Depth (AOD), which models the extinction of light in the atmosphere due to aerosols. This parameter depends on highly variable factors such as atmospheric humidity and the concentration of dust or pollutants suspended in the air. Accurately determining the AOD *a priori* is challenging, as it would require precise meteorological measurements at the sensor location and time of observation. Consequently, the proposed methodology estimates the satellite attitude under conditions of unknown optical properties and AOD, a task complicated by the inherent ambiguity of the measurement, whereby multiple combinations of attitude, optical, and atmospheric parameters can result in similar light curves. To address this, the approach integrates statistical inference with optimisation and data analysis techniques to ensure accurate and robust estimation of the unknown parameters. Developed with operational applicability in mind, the methodology enables precise attitude estimation within minutes. Its performance is validated through a realistic test case, demonstrating its suitability for real-world operational scenarios.

1. INTRODUCTION

Traditional Space Surveillance and Tracking (SST) methods rely on sensor measurements —typically from telescopes and radars— for cataloguing space objects in Earth's orbits. These measurements also form the basis of the orbit determination and propagation processes, whose accuracy is critical for enabling subsequent SST activities such as conjunction detection, collision risk assessment, collision avoidance, re-entry prediction, visibility analysis, and sensor planning. However, the technological advancements that have given rise to the New Space era have led to an exponential increase in space traffic, with numerous actors from diverse scientific, commercial, and military sectors now accessing space. As a result, traditional SST activities must be adapted to this evolving environment, where orbit determination alone is no longer sufficient to ensure the safety and security of space operations. Instead, a comprehensive characterisation of space objects —including their geometric and optical properties, attitude, and mission capabilities— is required to protect space assets and to support the long-term sustainability of the space environment by mitigating the proliferation of space debris.

Copyright © 2025 Advanced Maui Optical and Space Surveillance Technologies Conference (AMOS) – www.amostech.com

In this context, estimating the attitude of space objects is of paramount importance across a wide range of civil activities, including space object correlation and cataloguing, improving the estimation of collision probabilities and re-entry predictions, and designing space debris mitigation missions like Active Debris Removal (ADR) and In-Orbit Servicing (IOS). Additionally, it has strategic importance in military applications, where detailed knowledge of other satellites' missions and capabilities is essential. Beyond attitude, the optical reflective properties of a space object's surfaces are critical, as they significantly influence solar radiation pressure, a major perturbation force that must be accurately accounted for in orbital propagation and subsequent operations. This consideration is particularly relevant given the wide diversity of aerospace materials and the fact that, even when the materials constituting a space object are known, prolonged exposure to the space environment unpredictably alters their optical properties.

One of the most cost-effective methods for estimating unknown characteristics of space objects is the use of light curves, that is, the temporal evolution of photometric measurements taken by ground-based telescopes, in a strategy known as light curve inversion. However, this problem is inherently challenging due to several factors, primarily the typically non-Gaussian and multimodal probability density function associated with the unknown attitude and/or physical parameters. This complexity arises from the highly non-linear measurement model, which must account for specular reflections and self-shadowing interactions between different components of the space object, as well as the intrinsic measurement ambiguity, namely the existence of multiple combinations of attitude and/or physical parameters that produce equivalent photometric signatures.

The strong coupling between attitude, optical, and geometric parameters has led to the development of methodologies that typically assume knowledge of all but one of these parameter types. Over the past decade, various attitude estimation techniques have been proposed under the assumption of perfect knowledge of the geometric and optical properties of the space object. Initial efforts employed the Least Squares Method (LSM) [1][2] and the Unscented Kalman Filter (UKF) [3][4] to solve the light curve inversion problem. However, these estimation methods were soon abandoned because they depend on precise initial estimates and are unsuitable for non-Gaussian, multimodal probability density functions. The current state of the art is based on methods capable of exploring the full solution space and handling the complexities of the probability distribution, primarily sequential Bayesian estimation techniques, including particle filters [4]-[8] and Gaussian mixture models [9][10], as well as optimisation algorithms, particularly Particle Swarm Optimisation (PSO) [11]-[15]. A promising approach is also presented in [16], based on Adaptive Importance Sampling (AIS) principles and integrating resampling strategies with PSO.

Regarding attitude estimation methods that are independent of physical parameters, the approach proposed in [1] does not require any prior knowledge of the object's shape. However, it imposes a restrictive condition on the relative position between the Sun, the space object, and the sensor, which significantly limits its operational applicability. More recently, an attitude estimation method using an observation model that does not require knowledge of the optical parameters is introduced in [17], using Gaussian Process Regression (GPR), a machine learning technique. However, the training dataset depends on both the object shape and the observation conditions, which can vary infinitely. Consequently, research efforts have predominantly focused on the simultaneous estimation of attitude and physical parameters, as both are fundamental to the effective execution of other SST activities due to their direct impact on drag force and solar radiation pressure.

In this research line, [18] presents a Multiple-Model Adaptive Estimation (MMAE) approach based on the UKF to estimate rotational and translational states using multiple candidate shape models, providing a probabilistic metric of each shape model's contribution to the final estimate. Moreover, a Sampling Importance Resampling (SIR) particle filter is employed in [19] to track the attitude of space objects under uncertainty in surface parameters, including the surface area, the relative diffuse/specular weighting factor, the diffuse albedo, and the microfacet slope. Other studies have attempted to estimate surface parameters explicitly, typically within constrained tracking scenarios. For example, [4] uses a SIR particle filter, while [20] combines a particle filter with an expectation-maximisation clustering algorithm to approximate the state distribution using Gaussian mixture models. As an alternative to particle filters, the Adaptive Hamiltonian Markov Chain Monte Carlo (AHMC) method introduced in [21] generates samples from the posterior probability density function using relatively simple proposal and rejection rules. Applied to a model comprising four surfaces under simplified observation conditions, it successfully estimates the diffuse albedo-area product and two parameters defining surface orientation. Finally, Particle Swarm Optimisation (PSO) has also been investigated for the simultaneous estimation of attitude and optical properties in [22], reporting promising performance metrics.

Copyright © 2025 Advanced Maui Optical and Space Surveillance Technologies Conference (AMOS) – www.amostech.com

It is important to note that the previous studies have primarily focused on rotating objects or have assumed simplified observation geometries without fully accounting for the orbital motion of space objects. Consequently, none address the challenges posed by three-axis stabilised satellites, which exhibit lower variation in the relative position between the Sun, the space object, and the sensor, leading to increased measurement ambiguity. This study aims to fill this gap by simultaneously estimating the attitude and optical properties of three-axis stabilised satellites with known shape, under the worst-case scenario in which no prior knowledge of the unknown parameters is available and only photometric measurements from a single sensor are used. Additionally, the influence of atmospheric conditions at the sensor location on the observed irradiance is considered, with particular focus on the Aerosol Optical Depth (AOD), which depends on the aerosol concentration and exhibits significant variability, complicating real-time operations. Considering these factors, a novel approach is proposed to provide an accurate, robust, and computationally efficient solution applicable to real operational scenarios.

2. METHODOLOGY

2.1 Observation model

Solving the light curve inversion problem requires a measurement model capable of simulating photometric observations at the times of the actual measurements. In this work, the light curve simulator ***Grial*** [16] is employed. ***Grial*** uses OpenGL to graphically compute the contribution of each illuminated and visible surface pixel of the space object model to the reflected light, achieving an average simulation time of 1.4 ms per observation. Full details of the observation model implemented in ***Grial*** are provided in [16]. In summary, the model relies on a realistic bidirectional reflectance distribution function (BRDF), which describes how sunlight is reflected from the surfaces of the space object. Specular reflections are modelled using the Cook-Torrance BRDF [23], with the Fresnel factor computed using Schlick's approximation [24], and the GGX model [25] applied to represent the microfacet slope distribution. The diffuse component of the BRDF is described using the Lommel-Seeliger reflectance model [26]. Additionally, ***Grial*** accounts for self-shadowing effects caused by different components of the space object.

Once the irradiance detected by the sensor I_o is determined, the apparent magnitude of the space object can be computed as:

$$m = -2.5 \log\left(\frac{I_o}{I_{ref}}\right) + T_{atm} \tag{1}$$

where $I_{ref} = 2.518 \times 10^{-8}$ W/m^2 corresponds to the zero point of the apparent bolometric magnitude scale, and T_{atm} is an atmospheric transmission factor that accounts for the light extinction caused by the Earth's atmosphere. The model described in [27] is adopted to consider the primary atmospheric sources of light attenuation, namely Rayleigh scattering by air molecules, ozone absorption, and scattering by aerosols suspended in the atmosphere.

$$T_{atm} = T_{Ray} + T_{O_3} + T_{aod} \tag{2}$$

The attenuation of light due to Rayleigh scattering T_{Ray} and ozone absorption T_{O_3} can be calculated with good accuracy using the analytical expressions provided in [27]. In contrast, the attenuation caused by aerosol scattering is governed by the Aerosol Optical Depth (AOD), which depends on the optical thickness of atmospheric aerosols at a wavelength of 550 nm. Due to its high variability, accurate determination of the AOD requires local meteorological measurements at the sensor site. Once obtained, the attenuation caused by aerosol scattering can be computed as [27]:

$$T_{aod} = 2.5 m_{air} \log[\exp(aod)] \tag{3}$$

$$aod = aod_{550}\left(\frac{\lambda}{\lambda_{ref}}\right)^{-1.3} \tag{4}$$

where λ is the mean wavelength of light, $\lambda_{ref} = 550$ nm is the reference wavelength, and m_{air} is the air mass between the sensor and the space object, which can be computed using Rozenberg's formula [28].

Copyright © 2025 Advanced Maui Optical and Space Surveillance Technologies Conference (AMOS) – www.amostech.com

2.2 Light curve inversion method

This section describes the proposed light curve inversion method. As previously outlined, the objective is to estimate the attitude and the optical properties of three-axis stabilised satellites with known shape. Given the difficulty of obtaining accurate Aerosol Optical Depth (AOD) measurements at the sensor location, the AOD is also estimated as part of the process. The methodology is developed to address the most challenging scenario, where only photometric measurements from a single sensor are available, and no prior knowledge exists of the satellite's attitude, the diffuse optical properties of its main body surfaces, or the AOD at the sensor location. Moreover, the method is designed for operational applicability, prioritising accuracy and robustness while preserving computational efficiency.

The proposed light curve inversion method employs Bayesian inference to estimate the unknown state parameters from the observed light curve. To achieve the stated objectives, it integrates different estimation, optimisation, and data analysis techniques. An overview of the complete light curve inversion algorithm is presented in Figure 2-1. As shown, the method begins by processing the light curve data and initialising the proposal distribution for the attitude parameters. This is followed by an iterative process, whose key steps include the estimation of optical and atmospheric parameters for each candidate attitude state, the reconstruction of the simulated measurements using the estimated parameters, the evaluation of quality metrics for each candidate solution, and the subsequent application of adaptive processes such as Adaptive Particle Allocation, Systematic Resampling, and Particle Swarm Optimisation to progressively refine the proposal distribution. The procedures related to the estimation of attitude parameters are detailed in Section 2.2.1, while the estimation of the optical properties and the AOD is described in Section 2.2.2.

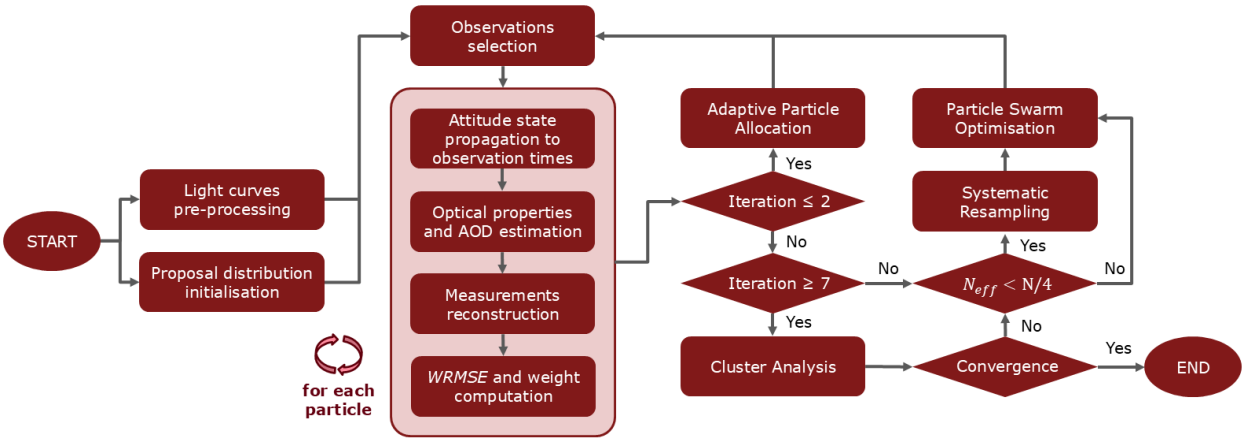

Figure 2-1. Light curve inversion method

2.2.1 Attitude estimation

The method developed for attitude estimation is based on the principles of Adaptive Importance Sampling (AIS) [29]. Considering a vector of unknown static attitude parameters $\boldsymbol{x}$ with an unknown probability density function $\pi(\boldsymbol{x})$, AIS methods approximate this target distribution by drawing samples from a proposal distribution $q(\boldsymbol{x})$. Specifically, AIS methods typically consist of three fundamental steps, performed iteratively until convergence is achieved: sampling from the proposal distribution, computing the importance weights for each sample, and updating the proposal distribution for the next iteration. The importance weight assigned to each sample quantifies its contribution to the approximation of the target distribution. In the context of Bayesian inference, the importance weight function can be computed as:

$$w(\boldsymbol{x}) = \frac{\pi(\boldsymbol{x})}{q(\boldsymbol{x})} = \frac{\ell(\boldsymbol{z}|\boldsymbol{x})p_0(\boldsymbol{x})}{q(\boldsymbol{x})} \tag{5}$$

where $\boldsymbol{z}$ is a vector of observed data, and the target distribution $\pi(\boldsymbol{x})$ is expressed in terms of the likelihood function $\ell(\boldsymbol{z}|\boldsymbol{x})$, and the prior probability density function $p_0(\boldsymbol{x})$ in accordance with Bayes' theorem.

Copyright © 2025 Advanced Maui Optical and Space Surveillance Technologies Conference (AMOS) – www.amostech.com

To mitigate the impact of measurement ambiguities during the estimation process, the observed photometric data are processed using a batch strategy, wherein a group of measurements is used at each iteration of the proposed light curve inversion method. Accordingly, one of the initial steps in the methodology involves the pre-processing of the observed light curves to prepare the selection of measurements for each iteration. The observed light curve is first divided into a number of sub-tracks equal to the number of photometric observations required per iteration. Then, at each iteration, one measurement is selected from each sub-track. This strategy ensures that each batch contains measurements acquired at different elevation angles from the ground station, which facilitates the estimation of the AOD, as it depends on the air mass between the sensor and the satellite (see Equation (3)). Experimental results indicate that using 60 measurements per iteration provides sufficient accuracy for solving the light curve inversion problem while maintaining computational efficiency.

A consequence of the batch-processing strategy for photometric measurements is that the particle quality metric must be capable of handling observations from different sensors with varying noise levels. To address this, the weighted root mean square error ($WRMSE$) is adopted as particle quality metric:

$$WRMSE = \sqrt{\frac{1}{K}\sum_{j=1}^{K}\left(\frac{y_j - z_j}{\sigma_{s,j}}\right)^2} \tag{6}$$

where z_j is a real photometric observation, y_j is the corresponding simulated measurement for a given particle state at the time of observation, and $\sigma_{s,j}$ denotes the standard deviation of the sensor noise associated with measurement z_j.

The normalised weight of each particle can then be computed by mapping the $WRMSE$ to a probability using a softmax function. This is done by applying Equation (5) and assuming that the importance density is equal to the prior density at each iteration of the AIS method, i.e. $q(\boldsymbol{x}) = p_0(\boldsymbol{x})$:

$$\bar{w}_i = \ell\left(\{z_j\}_{j=1}^{K}\middle|\boldsymbol{x}_i\right) = \frac{\exp(-WRMSE_i^2)^{1/T}}{\sum_{i=1}^{N}\exp(-WRMSE_i^2)^{1/T}} \tag{7}$$

where the likelihood function represents the probability of observing the given set of photometric measurements conditioned on a specific particle state.

As shown in Equation (7), a temperature parameter T is incorporated into the particle weight formulation to implement Simulated Annealing [30][31]. This strategy aims to reduce the risk of premature convergence to local optima, particularly when Systematic Resampling is applied during the early stages of the light curve inversion method. The rationale for this approach arises from the relative nature of particle-based estimation methods, which assess each particle's quality in comparison with others. Such relative evaluation can be problematic when multiple strong local optima are present, as in the current application. In the proposed method, in addition to the inherent measurement ambiguities of the light curve inversion problem, the presence of local optima is further compounded by the fact that, for each candidate attitude state (i.e. for each particle), the diffuse reflective properties and the AOD are estimated by solving a least-squares optimisation problem using a reduced subset of photometric measurements, as explained in Section 2.2.2.

Simulated Annealing is therefore applied during the initial iterations of the light curve inversion method. Specifically, the temperature parameter decreases linearly from 5 to 1 over the first five iterations following the completion of the Adaptive Particle Allocation process. This strategy is particularly important when no prior knowledge of the object's attitude exists and the method is initialised with a uniform particle distribution, as it flattens the weight distribution in the early stages, promoting broader exploration of the search space guided by the Particle Swarm Optimisation algorithm. As the temperature approaches unity, the weighting sharpens, allowing particles with lower $WRMSE$ to dominate the distribution. Consequently, Systematic Resampling replicates the best-performing particles more aggressively, concentrating them in the most promising regions of the solution space for their local exploration and refinement in subsequent iterations.

Copyright © 2025 Advanced Maui Optical and Space Surveillance Technologies Conference (AMOS) – www.amostech.com

The remaining step of the AIS strategy is the update of the proposal distribution from one iteration to the next. The light curve inversion method presented in this work employs a combination of techniques to introduce a novel adaptive approach, specifically designed to address the challenges of the light curve inversion problem in an operational context. The objective is to reduce the computational cost associated with reconstructing the proposal probability distribution at each iteration, which is needed to draw samples for the next iteration. The techniques that enable an implicit estimation of the target probability distribution are described below, along with the cluster analysis used to assess convergence and identify the most probable solution.

a) Adaptive Particle Allocation

An adaptive allocation of particles is carried out during the first two iterations of the light curve inversion method to refine the initial proposal distribution. This process involves reallocating particles from low-probability regions to areas of higher probability. In particular, particles with a $WRMSE$ in the upper tertile of the $WRMSE$ distribution are repositioned in the vicinity of the best-performing particles. Their new locations are determined using the sampling step of the initial proposal distribution, ensuring they are placed at intermediate positions between existing particles to improve the initial exploration of the solution space.

b) Cluster Analysis

Clustering is a technique used to group similar data points based on shared characteristics. The proposed light curve inversion method employs Density-Based Spatial Clustering of Applications with Noise (DBSCAN) [32], a density-based algorithm that identifies clusters according to the concentration of data points. Cluster analysis is thus used to identify the modes of the target probability distribution, assess the convergence of the estimation process, and compute the most likely solution within each cluster along with its associated standard deviation.

The DBSCAN implementation from the Hipparchus library [33] is employed in this work. However, due to the presence of different types of unknown parameters —orientation angles, reflection coefficients, and the AOD— a customised distance metric is incorporated into the DBSCAN algorithm. This metric is defined as the average Manhattan distance computed across all parameters. It is normalised using half the sampling step of the initial proposal distribution for the attitude parameters, and half the parameter range for the optical and atmospheric parameters, which are constrained to the interval [0,1]. Furthermore, the DBSCAN algorithm requires two threshold values to identify clusters of particles: the minimum number of points required to form a cluster, and the neighbourhood radius. These parameters have been determined empirically, adopting conservative values. Specifically, the minimum cluster size set to 10 % of the total number of particles, and the neighbourhood radius is set to 0.1 in terms of the average normalised Manhattan distance.

The cluster analysis is performed from the seventh iteration onwards, after the Simulated Annealing process has concluded, as it is computationally intensive. This delay allows particles a few iterations to move towards high-probability regions. Two criteria are defined to assess the convergence of the light curve inversion method:

- Global criterion: at least 80 % of the particles must be assigned to a cluster.
- Local criterion: the $WRMSE$ associated with the weighted state estimate of each cluster must be below 1.1, and the relative change in $WRMSE$ between consecutive iterations must be less than 5 %.

The local criterion is evaluated after refining the weighted average parameters of each cluster through a two-step optimisation process. Initially, the optical and the atmospheric parameters are refined using the Least Squares Method (LSM) described in Section 2.2.2, applied to an extended set of measurements obtained by sampling the observed light curve at one-second intervals. Subsequently, the weighted average attitude state, together with the refined optical and atmospheric parameters, is further optimised using Powell's Bound Optimization BY Quadratic Approximation (BOBYQA) algorithm [34], as implemented in the Hipparchus library [35], to minimise the $WRMSE$ with respect to the extended dataset of observed measurements. This two-step optimisation process is justified for several reasons: the weighted average optical and atmospheric parameters are not expected to be accurate since only 60 measurements are used in each iteration; the BOBYQA algorithm is sensitive to local minima if the initial estimate of the optical and atmospheric parameters is not sufficiently precise; and, contrary to the optical and atmospheric parameters, no analytical partial derivatives are available for the attitude parameters, while numerical partial derivatives are often unstable and expensive to compute.

Copyright © 2025 Advanced Maui Optical and Space Surveillance Technologies Conference (AMOS) – www.amostech.com

If convergence of the light curve inversion method is not achieved, the proposal distribution must be updated for the subsequent iteration. As previously discussed, this is accomplished through the combined use of Systematic Resampling and Particle Swarm Optimisation, which reduces the computational cost and accelerates convergence towards the most promising candidate solutions. The refined attitude state of each cluster is incorporated into the particle set for use in subsequent iterations by replacing the particles with the highest $WRMSE$.

c) Systematic Resampling

Systematic Resampling [36] is commonly employed to mitigate particle degeneracy, a condition in which a small subset of particles carries most of the weight, while the majority contribute negligibly to the overall estimate. This resampling step is triggered when the effective sample size [37], given by Equation (8), falls below 25 % of the total number of particles:

$$N_{eff} = \frac{1}{\sum_{i=1}^{N} \bar{w}_i^2} \tag{8}$$

The application of Systematic Resampling not only reduces the computational cost associated with updating low-weight particles, but also improves the convergence of the light curve inversion method when used in conjunction with Particle Swarm Optimisation. It is particularly effective at removing particles from regions that initially appeared to have high probability but become less relevant as the estimation process progresses. This reallocation typically occurs as new photometric measurements are incorporated, and the estimation of the true optimal solution is progressively refined.

d) Particle Swarm Optimisation

Particle Swarm Optimisation (PSO) [38] is a population-based global optimisation algorithm that, in this context, is used to assist in the implicit estimation of the target probability distribution, avoiding the computational cost of explicitly computing it at each iteration. In addition, PSO provides a more efficient alternative to traditional techniques commonly employed in particle filters to preserve particle diversity, such as the injection of artificial noise, enabling faster convergence to the correct attitude solutions.

In PSO, particles move through the search space according to their momentum, which is updated iteratively based on both their own experience and that of their neighbours. Let the j-th component of the i-th particle's position and velocity vectors at iteration k be denoted as $x_{i,j}^k$ and $v_{i,j}^k$, respectively. Each scalar state parameter and its corresponding velocity are then updated according to the following equations [39]:

$$\begin{gathered} v_{i,j}^k = w v_{i,j}^{k-1} + c_1 r_1 \left(x_{i,j}^{pbest} - x_{i,j}^k\right) + c_2 r_2 \left(x_j^{gbest} - x_{i,j}^k\right) \\ x_{i,j}^k = x_{i,j}^{k-1} + v_{i,j}^k \end{gathered} \tag{9}$$

where w is the inertia weight factor, c_1 is the cognitive coefficient, $x_{i,j}^{pbest}$ is the j-th component of the best state found by the i-th particle (personal best), c_2 is the social coefficient, x_j^{gbest} is the j-th component of the best state found by any particle in the swarm (global best), and r_1 and r_2 are random numbers drawn from $U(0,1)$.

The PSO parameters are selected to first encourage local exploration during the initial iterations of the light curve inversion method and, as the process advances, to promote exploitation by accelerating the convergence of particles towards globally optimal states. To achieve this, the inertia weight and the cognitive coefficient are decreased linearly, while the social coefficient is increased linearly as the iterations progress. The parameter values, determined experimentally, are set to $w_{min} = 0.2$, $w_{max} = 0.4$, $c_{1,min} = c_{2,min} = 0.5$, $c_{1,max} = c_{2,max} = 2.5$. The linear variation of these parameters is applied during the same iterations in which Simulated Annealing is active, beginning after the conclusion of the Adaptive Particle Allocation process and lasting for $K = 5$ iterations. For all subsequent executions of PSO, the parameter values from iteration K are retained.

Copyright © 2025 Advanced Maui Optical and Space Surveillance Technologies Conference (AMOS) – www.amostech.com

Regarding the first execution of PSO, if Equation (9) were applied directly to compute the velocity, it would depend solely on the global best state, since the particles have no prior velocity and their personal best state coincides with their current state. This can be problematic in the context of the light curve inversion method, as the $WRMSE$ of the particles is computed using the optical properties and AOD that minimise the $WRMSE$ with respect to the photometric measurements selected in each iteration, which may lead to convergence to local optima. Therefore, to reduce reliance on the global best state and to promote local exploration of the solution space during the early iterations of the light curve inversion method, the particle velocity is computed according to the following equation in the first execution of the PSO:

$$v_{i,j}^{k=1} = c_{2,min} r_2 \left(x_j^{gbest} - x_{i,j}^{k=1} \right) + r_3 \Delta_{i,j} \tag{10}$$

where $c_{2,min} = 0.5$, $r_2 \sim U(0,1)$, $r_3 \sim U(-1,1)$, and $\Delta_{i,j}$ is the exploratory step computed as follows:

$$\Delta_{i,j} = \Delta_{j,min} + \eta_i \left(\Delta_{j,max} - \Delta_{j,min} \right) \tag{11}$$

$$\eta_i = \frac{WRMSE_i^* - WRMSE_{min}}{WRMSE_{Q3} - WRMSE_{min}} \tag{12}$$

Here, $\Delta_{j,max}$ is half the sampling step of the initial uniform proposal distribution for the j-th state parameter, and $\Delta_{j,min} = \Delta_{j,max}/2$. The parameter $\eta_i \in [0,1]$ represents a particle performance score. $WRMSE_{min}$ is the minimum $WRMSE$ across the swarm, while $WRMSE_{Q3}$ denotes the third quartile of the $WRMSE$ distribution. The value $WRMSE_i^* = \min \left\{ WRMSE_i, WRMSE_{Q3} \right\}$ clamps the actual $WRMSE$ of the i-th particle, $WRMSE_i$, to the upper quartile value to mitigate the influence of outliers.

Finally, it is important to bear in mind that the target probability distribution is likely to be multimodal. Therefore, the PSO must maintain a set of global best states, which is updated at each iteration based on two criteria that must be satisfied simultaneously:

- Selected particles must have a $WRMSE$ within the lowest tertile of the current iteration's $WRMSE$ distribution. Replicated particles resulting from the resampling step, if any, are considered only once. Global best states from the previous iteration that meet this $WRMSE$ threshold are also retained.
- Only the particle with the lowest $WRMSE$ within a defined neighbourhood is selected. Neighbourhoods are defined under the assumption that different attitude solutions cannot exist within an angular separation of 30 deg. Two particles are considered to belong to the same neighbourhood if the angular distance between their respective attitude states is less than this threshold.

At each iteration of the PSO, the velocity of each particle is updated considering its nearest global best state, which is identified using the Manhattan distance calculated across all attitude parameters while appropriately accounting for the periodic nature of some of them.

2.2.2 Optical properties and AOD estimation

This section outlines the principal characteristics of the proposed method for estimating the optical parameters of satellite surfaces and the Aerosol Optical Depth (AOD) at the sensor location. Specifically, the diffuse reflectance coefficient of all materials comprising the satellite's main body is estimated. The methodology is based on two key assumptions, considered reasonable in light of previous studies. Firstly, all materials constituting the main body are assumed to behave as purely diffuse reflectors. This assumption is supported by the work in [40], where it is demonstrated that the dominant factor influencing the reflectance spectra of three-axis stabilised GEO satellites is the presence of multi-layer insulation (MLI) on the platform surface. Secondly, when present, the solar arrays are modelled as purely specular reflectors, consistent with previous studies [41][42], which indicate that solar arrays exhibit an albedo of approximately 0.1 with minimal dispersion.

Copyright © 2025 Advanced Maui Optical and Space Surveillance Technologies Conference (AMOS) – www.amostech.com

The estimation of the diffuse optical properties of the materials composing the surfaces of the satellite, as well as the AOD at the sensor location, is performed using a Least Squares Method (LSM). Specifically, the Levenberg-Marquardt algorithm [43][44], as implemented in the Hipparchus library [45], is used to solve the non-linear least squares problem. As indicated in Figure 2-1, this estimation is carried out for each particle at every iteration of the light curve inversion method. Once the diffuse reflection coefficients and the AOD have been estimated, the simulated measurements are reconstructed at the times corresponding to the selected actual observations, enabling the computation of the particle quality metrics. The Levenberg-Marquardt algorithm is selected because the observation model provided in Equations (1)-(4) can be expressed analytically in terms of the $k_{d,\Gamma}$ and aod parameters as follows, and it is a more computationally efficient method than derivative-free algorithms:

$$m = -2.5 \log\left(\sum_{\Gamma} C_{\Gamma} k_{d,\Gamma} + \frac{I_{o,array}}{I_{ref}}\right) + \frac{2.5 m_{air}}{\ln 10} aod + T_{Ray} + T_{O_3} \tag{13}$$

$$C_{\Gamma} = \frac{I_i}{2\pi r^2 I_{ref}} \sum_{\gamma \in \Gamma} A_{\gamma} \frac{(\boldsymbol{l} \cdot \boldsymbol{n})_{\gamma} (\boldsymbol{v} \cdot \boldsymbol{n})_{\gamma}}{(\boldsymbol{l} \cdot \boldsymbol{n} + \boldsymbol{v} \cdot \boldsymbol{n})_{\gamma}} \tag{14}$$

where the subscript Γ refers to surface components of the satellite that share the same diffuse reflective coefficient $k_{d,\Gamma}$, while the subscript γ denotes the facets into which each surface Γ is divided to compute its contribution to the reflected light. The term $I_{o,array}$ represents the observed irradiance from the satellite's solar arrays, if present. The constant associated with each surface diffuse reflection coefficient C_{Γ} is obtained from the diffuse BRDF of the Lommel-Seeliger model [26] and the expression of the total observed irradiance detected by the sensor [16]. This constant depends on the irradiance received from the Sun by the satellite I_i, the distance from the satellite to the sensor r, and facet-specific parameters, namely the area A_{γ}, the unit normal vector $\boldsymbol{n}_{\gamma}$, and the unit vectors in the direction of the light source $\boldsymbol{l}_{\gamma}$ and the sensor $\boldsymbol{v}_{\gamma}$. In this work, the worst-case scenario, in which only photometric measurements from a single sensor are available, is considered. Nevertheless, the formulation can be readily extended to incorporate measurements from multiple sensors or different observation windows by estimating the AOD at each sensor location and for each time window.

Since the domains of the unknown parameters $k_{d,\Gamma}$ and aod are constrained to the interval $[0,1]$, applying an unconstrained optimisation algorithm like Levenberg-Marquardt can be problematic. This issue is effectively addressed through a reparametrisation strategy, in which each constrained parameter is expressed as a smooth, differentiable function of an unconstrained variable. The standard logistic function is particularly well-suited for this purpose, as it maps the entire set of real numbers $\mathbb{R}$ onto the open interval $(0,1)$, naturally enforcing the lower and upper bounds of the optical and atmospheric parameters.

$$\sigma(u) = \frac{1}{1 + \exp(-u)} \tag{15}$$

Therefore, the Levenberg-Marquardt method operates on the unconstrained variables, which are related to the constrained parameters through the transformations $k_{d,\Gamma} = \sigma\left(u_{k_{d,\Gamma}}\right)$ for the diffuse reflection coefficient of surface Γ, and $aod = \sigma(u_{aod})$ for the AOD at the sensor location.

Moreover, the residual function used to solve the least-squares problem with the Levenberg-Marquardt algorithm is defined as the difference between the observed apparent magnitude m_{obs} and the simulated measurement m_{sim}, as given by Equation (13). This difference is normalised by the standard deviation of the sensor noise σ_s, thereby expressing the residual in units of measurement uncertainty. Such normalisation improves both the accuracy and robustness of the estimation, particularly when incorporating photometric measurements from different sensors.

$$\epsilon = \frac{m_{obs} - m_{sim}}{\sigma_s} \tag{16}$$

Finally, the partial derivatives of the residual with respect to the unconstrained parameters, which constitute the Jacobian matrix, are given by:

Copyright © 2025 Advanced Maui Optical and Space Surveillance Technologies Conference (AMOS) – www.amostech.com

$$\frac{\partial \epsilon}{\partial u_{k_{d,\Gamma}}} = \frac{-2.5 C_\Gamma k_{d,\Gamma}\left(1 - k_{d,\Gamma}\right)}{\left(\sum_\Gamma C_\Gamma k_{d,\Gamma} + \frac{I_{o,array}}{I_{ref}}\right)\sigma_s \ln 10} \tag{17}$$

$$\frac{\partial \epsilon}{\partial u_{aod}} = \frac{2.5 m_{air} aod(1 - aod)}{\sigma_s \ln 10} \tag{18}$$

3. RESULTS

This section presents the results of the analysis conducted to evaluate the performance of the proposed light curve inversion method. The objective is to estimate the attitude parameters and the optical reflective properties of a three-axis stabilised satellite with a known shape, as well as the AOD at the sensor location. Specifically, the satellite follows an inertial pointing law, and the attitude parameters are expressed as Euler angles (yaw ψ, pitch θ, and roll ϕ), which define the rotation of a body-fixed reference frame B, attached to the space object, relative to an inertial reference frame, the Geocentric Celestial Reference Frame (GCRF), following the ZYX convention. Regarding the satellite's optical reflective properties, the analysis focuses on estimating the diffuse reflection coefficient of the different materials of the main body surfaces, according to the methodology explained in Section 2.2.2.

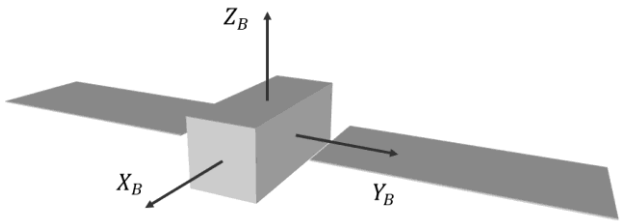

Figure 3-1. Satellite model

Table 3-1. Reference parameters

Attitude parameters	ψ [deg]	19
	θ [deg]	-6.5
	ϕ [deg]	37.5
Optical parameters	$k_{d,\pm X_B}$ [$-$]	0.8
	$k_{d,\pm Y_B}$ [$-$]	0.1
	$k_{d,\pm Z_B}$ [$-$]	0.45
Atmospheric parameter	aod [$-$]	0.2

The satellite model used in this study is shown in Figure 3-1 and consists of a quadrangular prism platform with dimensions $2.5 \times 1 \times 1$ m and a solar array measuring $1.5 \times 3.5 \times 0.01$ m, resulting in a total span of 9 m. The satellite is in a circular orbit at an altitude of 1000 km, with an orbital inclination of 20 deg and a right ascension of the ascending node of 0 deg. It is observed from a hypothetical optical sensor located at 5°N, 20ºE, 1600 m above mean sea level (WGS84). The reference attitude, optical and atmospheric parameters are provided in Table 3-1. These reference parameters generate the light curve shown in Figure 3-2, which serves as the reference light curve from which the unknown state parameters are estimated. The solar arrays are modelled as purely specular reflectors with a specular reflection coefficient of $k_s = 0.1$, and a roughness coefficient of $n_s = 0.1$ is used for all the materials. The reference light curve is simulated assuming sensor noise with a standard deviation of $\sigma_s = 0.1$ in apparent magnitude.

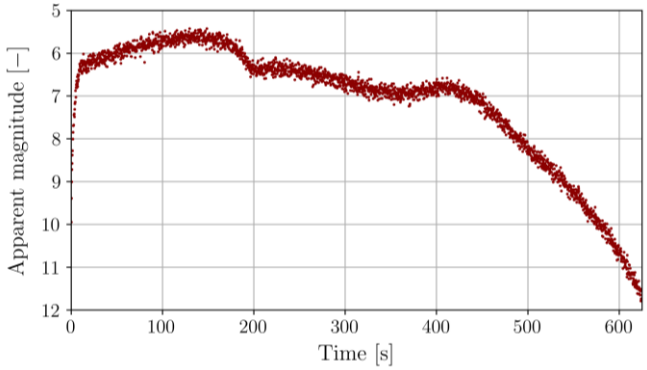

Figure 3-2. Reference light curve

Copyright © 2025 Advanced Maui Optical and Space Surveillance Technologies Conference (AMOS) – www.amostech.com

The execution of the light curve inversion method is described below. Figure 3-3 illustrates the distribution of particles within the solution space of the attitude parameters across different iterations. In all plots, the actual attitude state to be estimated is marked by a red cross. The process begins with the generation of a uniform distribution of particles, since no prior knowledge of the attitude is assumed. The sampling resolution was determined experimentally by analysing different test cases, and it was found that a step size of 18 deg provides a sufficiently fine discretisation to solve the light curve inversion problem accurately. In this test case, the solution space is constrained according to the symmetric geometric and optical properties of the satellite model, resulting in a total of 1000 particles.

The Adaptive Particle Allocation process is carried out during the first two iterations, and by the third iteration, regions of higher probability begin to emerge. Subsequent iterations focus on the local exploration of these regions, with particles progressively accelerating towards the most promising candidate solutions through the combined effects of Systematic Resampling and PSO. Notably, between the third and seventh iterations, convergence accelerates progressively, facilitated by the linear evolution of the PSO parameters and the temperature of the Simulated Annealing process. A cluster comprising 605 particles is identified for the first time at the eighth iteration, in which the absolute convergence criterion is already satisfied. The method requires until the tenth iteration to satisfy both the absolute and relative convergence criteria, ultimately achieving a final $WRMSE$ of 1.020 and a relative change of 1.39 % compared to the previous iteration.

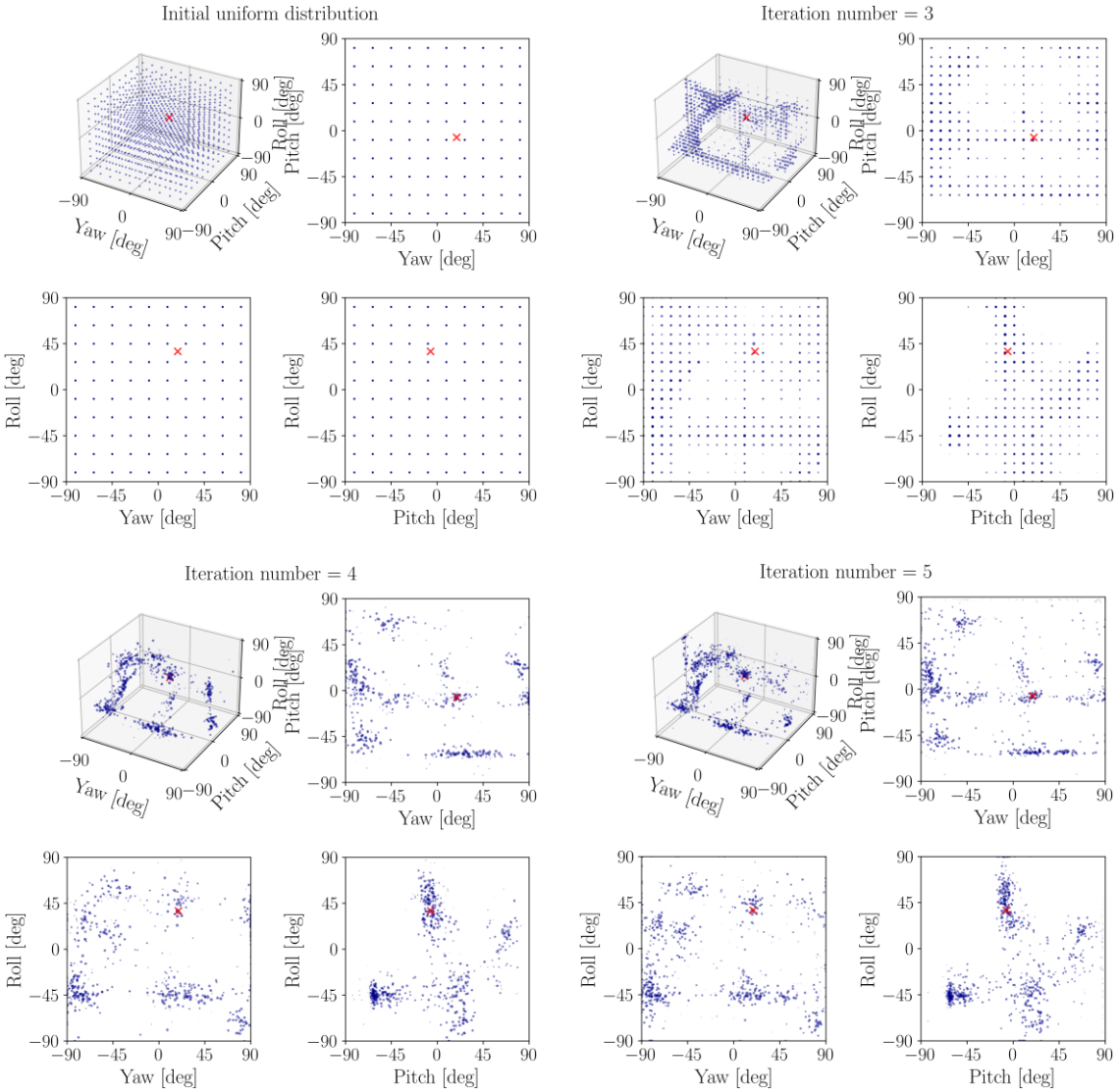

Copyright © 2025 Advanced Maui Optical and Space Surveillance Technologies Conference (AMOS) – www.amostech.com

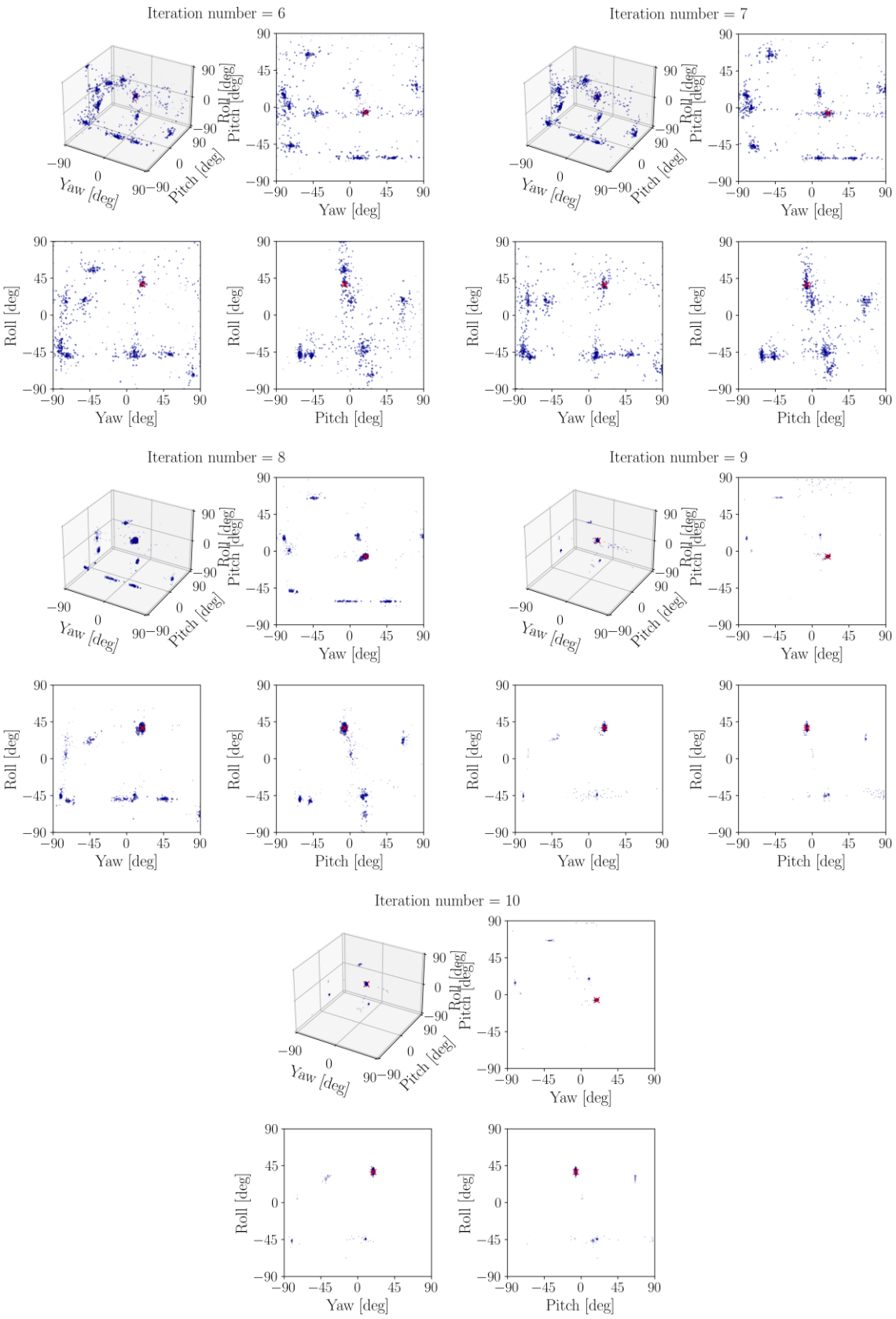

Figure 3-3. Execution of the light curve inversion method

Copyright © 2025 Advanced Maui Optical and Space Surveillance Technologies Conference (AMOS) – www.amostech.com

The numerical results at the iteration in which convergence is achieved are presented in Table 3-2. Specifically, the weighted average and standard deviation of the cluster are included, along with the final estimate of each parameter after the refinement step. The reference state is also provided to facilitate comparison. As observed, the weighted cluster state already offers a good estimate, particularly for the attitude parameters, since these are derived from the particle-based strategy. However, the diffuse reflection coefficients and the AOD show greater discrepancies relative to the reference values, likely due to the limited number of measurements used in the LSM at each iteration. The refinement step corrects these small deviations, reducing the $WRMSE$ and satisfying the convergence criteria.

Table 3-2. Results of the light curve inversion method

		Reference	Cluster estimate	Final estimate
Attitude parameters	ψ [deg]	19	18.789 ± 0.089	18.835
	θ [deg]	-6.5	-6.605 ± 0.061	-6.573
	ϕ [deg]	37.5	37.266 ± 0.331	37.427
Optical parameters	$k_{d,\pm X_B}$ [−]	0.8	0.782 ± 0.011	0.801
	$k_{d,\pm Y_B}$ [−]	0.1	0.012 ± 0.024	0.141
	$k_{d,\pm Z_B}$ [−]	0.45	0.519 ± 0.015	0.440
Atmospheric parameter	aod [−]	0.2	0.211 ± 0.008	0.205
$WRMSE$ [−]		−	1.254	1.020

The light curve corresponding to the final estimate is shown in Figure 3-4, alongside the reference light curve previously presented in Figure 3-5. An additional metric that complements the evaluation of the solution obtained is the set of residuals between each simulated measurement and the corresponding reference light curve value, normalised by the standard deviation of the sensor noise. These normalised residuals are presented in Figure 3-5, where it can be observed that the vast majority, specifically 95.84 % of the points, fall within the ± 2 range, indicating a high level of agreement between the simulated and the reference photometric measurements.

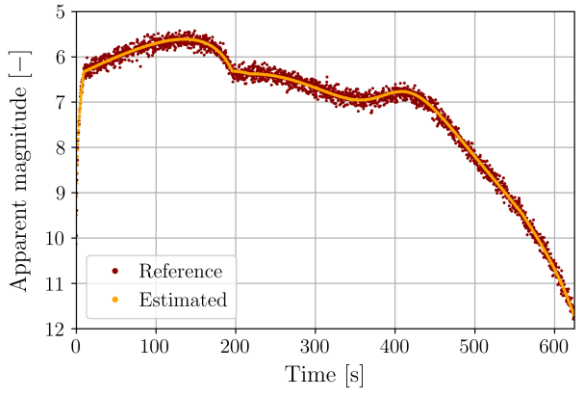

Figure 3-4. Reference and estimated light curves

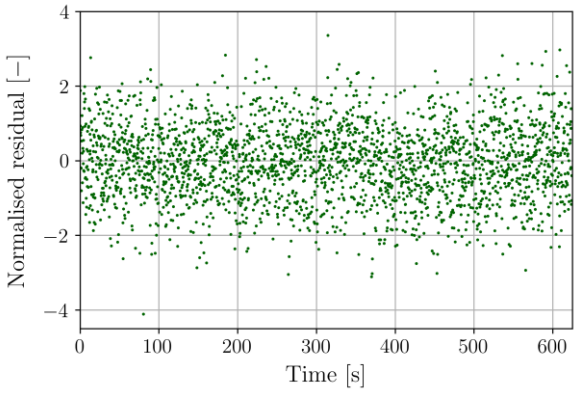

Figure 3-5. Normalised residuals

The computational cost associated with each process of the light curve inversion method is provided in Table 3-3. The analysis was performed on a computer equipped with an Intel(R) Core(TM) i7-10610U CPU @ 1.80 GHz, using 8 parallel threads, and an Intel(R) UHD Graphics GPU with 7.9 GB of memory. The reported results correspond to the average processing time per iteration for the 1000 particles used in the test case. The total time represents the duration required to achieve convergence. As it can be observed, the most computationally demanding step is the simulation of the photometric measurements, particularly due to the consideration of four distinct materials. However, the simulation of the measurements is fully parallelised, enabling a significant computational improvement to be readily achieved through the use of additional CPU cores. The second most time-consuming step is the refinement of the cluster estimate, primarily driven by the last optimisation stage performed using the BOBYQA algorithm.

Copyright © 2025 Advanced Maui Optical and Space Surveillance Technologies Conference (AMOS) – www.amostech.com

Table 3-3. Computational performance of the light curve inversion method

	Average time
Light curve pre-processing	0.014 s
Measurements simulation	110.3 s
LSM for $k_{d,\Gamma}$ and aod estimation	0.15 s
$WRMSE$ and weight computation	0.52 s
Adaptive Particle Allocation	0.28 s
Systematic Resampling	0.007 s
PSO	0.075 s
Clustering	1.55 s
Cluster refinement	40.5 s
Total	18.5 min

4. CONCLUSIONS

This study addresses the light curve inversion problem for the simultaneous estimation of the attitude and optical properties of three-axis stabilised satellites with known geometry. The formulation also incorporates the estimation of the Aerosol Optical Depth (AOD), an atmospheric parameter characterised by high variability that plays a critical role in shaping the photometric signature of space objects. The optical property estimation is limited to the diffuse reflection coefficients of the materials composing the satellite's main body, as previous studies have shown that specular reflections from the main body have a comparatively smaller influence on the light curve. Furthermore, solar arrays can be accurately modelled as purely specular reflectors. The joint estimation of attitude and optical properties improves other Space Surveillance and Tracking (SST) activities, since these parameters are instrumental in the characterisation of both atmospheric drag and solar radiation pressure effects.

The light curve inversion is performed using a novel methodology based on Bayesian inference, integrating estimation, optimisation, and data analysis techniques. The approach is specifically designed for operational applicability in real-world scenarios. Its performance is evaluated through a realistic test case representative of a situation in which the light curve inversion problem is solved to assess a satellite's deviation from its nominal attitude law. The results demonstrate excellent accuracy while maintaining computational efficiency. Potential lines for future work include the analysis of alternative attitude control modes, such as yaw-fixed or yaw-steering configurations, and the estimation of the specular contribution to the observed irradiance from the materials constituting the satellite's platform.

FUNDING

This project has received funding from the "Comunidad de Madrid" under the "Ayudas destinadas a la realización de doctorados industriales" program (project IND2023/TIC-28739).

REFERENCES

[1] D. Hall, J. Africano, D. Archambeault, B. Birge, D. Witte, and P. Kervin, "AMOS Observations of NASA's IMAGE Satellite," in *The 2006 AMOS Technical Conference Proceedings*, pp. 10–14, 2006.

[2] D. Hall, B. Calef, K. Knox, M. Bolden, and P. Kervin, "Separating Attitude and Shape Effects for Non-resolved Objects," in *The 2007 AMOS Technical Conference Proceedings*, pp. 464–475, 2007.

Copyright © 2025 Advanced Maui Optical and Space Surveillance Technologies Conference (AMOS) – www.amostech.com

[3] C. J. Wetterer and M. Jah, "Attitude determination from light curves," *Journal of Guidance, Control, and Dynamics*, vol. 32, no. 5, pp. 1648–1651, 2009.

[4] A. J. Bernard, "Attitude and Reflection Parameter Estimation of Resident Space Objects Using Ground-Based Photometry," *All Graduate Theses and Dissertations, Spring 1920 to Summer 2023*, no. 8187, 2021.

[5] R. Linares, J. Crassidis, and M. Jah, "Particle Filtering Light Curve Based Attitude Estimation for Non-Resolved Space Objects," *Advances in the Astronautical Sciences*, vol. 152, pp. 119–130, 2014.

[6] R. D. Coder, M. J. Holzinger, and R. Linares, "Three-Degree-of-Freedom Estimation of Agile Space Objects Using Marginalized Particle Filters," *Journal of Guidance, Control, and Dynamics*, vol. 41, no. 2, pp. 388–400, 2018.

[7] X. Du, Y. Wang, H. Hu, R. Gou, and H. Liu, "The Attitude Inversion Method of Geostationary Satellites Based on Unscented Particle Filter," *Advances in Space Research*, vol. 61, no. 8, pp. 1984–1996, 2018.

[8] Y. Wang, X. Du, R. Gou, Z. Liu, and H. Chen, "A Secondary Particle Filter Photometric Data Inversion Method of Space Object Characteristics," *Electronics*, vol. 12, no. 9, Article 2044, 2023.

[9] A. Burton and C. Frueh, "Two methods for light curve inversion for space object attitude determination," in *8th European Conference on Space Debris*, Apr. 2021.

[10] D. V. Cabrera, J. Utzmann, and R. Förstner, "The Adaptive Gaussian Mixtures Unscented Kalman Filter for Attitude Determination Using Light Curves," *Advances in Space Research*, vol. 71, no. 6, pp. 2609–2628, 2023.

[11] R. Clark, S. Dave, J. Wawrow, and R. Lee, "Performance of Parameterization Algorithms for Resident Space Object (RSO) Attitude Estimates," in *Proceedings of the Advanced Maui Optical and Space Surveillance Technologies*, Maui, HI, USA, pp. 15–18, 2020.

[12] A. Burton, L. Robinson, and C. Frueh, "Light Curve Attitude Estimation Using Particle Swarm Optimizers," *Advances in Space Research*, vol. 74, no. 11, pp. 5619–5638, 2024.

[13] S. Gagnon and J. L. Crassidis, "Particle Swarm Optimization on the Space of Quaternions with Applications to Attitude Estimation from Light Curves," *The Journal of the Astronautical Sciences*, vol. 72, no. 2, p. 8, 2025.

[14] L. Robinson and C. Frueh, "Optimal Light Curve Attitude Inversion with Measurement Noise: Two Case Studies," in *9th European Conference on Space Debris*, Apr. 2025.

[15] P. Bencivenga, G. Isoletta, R. Opromolla, and G. Fasano, "Integrating PSO and UKF for attitude estimation of Resident Space Objects via Light Curves," in *9th European Conference on Space Debris*, Apr. 2025.

[16] J. Rubio, A. de Andrés, C. Paulete, Á. Gallego, and D. Escobar, "Attitude Estimation of Uncontrolled Space Objects: A Bayesian-Informed Swarm Intelligence Approach," *Advances in Space Research*, in press.

[17] R. Hara, Y. Yoshimura, and T. Hanada, "Photometric Attitude Estimation using Gaussian Process Regression," in *Advanced Maui Optical and Space Surveillance (AMOS) Technologies Conference*, p. 96, 2024.

[18] R. Linares, J. Crassidis, M. Jah, and H. Kim, "Astrometric and Photometric Data Fusion for Resident Space Object Orbit, Attitude, and Shape Determination Via Multiple-Model Adaptive Estimation," in *AIAA Guidance, Navigation, and Control Conference*, Aug. 2010.

[19] M. J. Holzinger, K. T. Alfriend, C. J. Wetterer, K. K. Luu, C. Sabol, and K. Hamada, " Photometric Attitude Estimation for Agile Space Objects with Shape Uncertainty," *Journal of Guidance, Control, and Dynamics*, vol. 37, no. 3, pp. 921–932, 2014.

Copyright © 2025 Advanced Maui Optical and Space Surveillance Technologies Conference (AMOS) – www.amostech.com

[20] S. Yun and R. Zanetti, "Nonlinear Filtering of Light-Curve Data," *Advances in Space Research*, vol. 66, no. 7, pp. 1672–1688, 2020.

[21] R. Linares and J. Crassidis, "Space-Object Shape Inversion via Adaptive Hamiltonian Markov Chain Monte Carlo," *Journal of Guidance, Control, and Dynamics*, vol. 41, pp. 47–58, 2018.

[22] R. Clark, Y. Fu, S. Dave, and R. S. K. Lee, " Resident space object (RSO) attitude and optical property estimation from space-based light curves," *Advances in Space Research*, vol. 70, no. 11, pp. 3271–3280, 2022.

[23] R. L. Cook and K. E. Torrance, "A Reflectance Model for Computer Graphics," *ACM Transactions on Graphics*, vol. 1, no. 1, pp. 7–24, 1982, Association for Computing Machinery, New York, NY, USA.

[24] C. M. Schlick, "An Inexpensive BRDF Model for Physically-based Rendering," in *Computer Graphics Forum 13*, 1994.

[25] B. Walter, S. R. Marschner, H. Li, and K. E. Torrance, "Microfacet Models for Refraction Through Rough Surfaces," in *Proc. 18th Eurographics Conference on Rendering Techniques*, Goslar, DEU, Eurographics Association, pp. 195–206, 2007.

[26] M. B. Fairbairn, "Planetary Photometry: The Lommel-Seeliger Law," *Journal of the Royal Astronomical Society of Canada*, vol. 99, no. 3, pp. 92–93, 2005.

[27] C. Buil, "Le calcul de la transmission spectrale atmosphérique: application à la surveillance de l'activité Be d'étoiles faibles," http://www.astrosurf.com/aras/extinction/calcul.htm, accessed Dec. 19, 2024.

[28] G. V. Rozenberg, *Twilight: A Study in Atmospheric Optics*, New York: Plenum Press, 1966.

[29] M. F. Bugallo, V. Elvira, L. Martino, D. Luengo, J. Míguez, and P. M. Djuric, "Adaptive Importance Sampling: The Past, the Present, and the Future," *IEEE Signal Processing Magazine*, vol. 34, no. 4, pp. 60–79, 2017.

[30] S. Kirkpatrick, C. D. Gelatt Jr, and M. P. Vecchi, "Optimization by Simulated Annealing," *Science*, vol. 220, no. 4598, pp. 671–680, 1983.

[31] J. Deutscher, A. Blake, and I. Reid, "Articulated Body Motion Capture by Annealed Particle Filtering," in *Proceedings IEEE Conference on Computer Vision and Pattern Recognition (CVPR 2000)*, vol. 2, pp. 126–133, Jun. 2000, Cat. No. PR00662, IEEE.

[32] M. Ester, H.-P. Kriegel, J. Sander, and X. Xu, "A Density-Based Algorithm for Discovering Clusters in Large Spatial Databases with Noise," in *Proceedings of the Second International Conference on Knowledge Discovery and Data Mining*, pp. 226–231, 1996, AAAI Press.

[33] Hipparchus, "Cluster Algorithms," https://www.hipparchus.org/hipparchus-clustering/, accessed Dec. 17, 2024.

[34] M. J. D. Powell, "The BOBYQA Algorithm for Bound Constrained Optimization Without Derivatives," *Cambridge NA Report NA2009/06*, University of Cambridge, Cambridge, pp. 26–46, 2009.

[35] Hipparchus, "Class BOBYQAOptimizer," https://www.hipparchus.org/apidocs/org/hipparchus/optim/nonlinear/scalar/noderiv/BOBYQAOptimizer.html, accessed June 10, 2025.

[36] G. Kitagawa, "Monte Carlo Filter and Smoother for Non-Gaussian Nonlinear State Space Models," *Journal of Computational and Graphical Statistics*, vol. 5, no. 1, pp. 1–25, 1996.

[37] M. S. Arulampalam, S. Maskell, N. Gordon, and T. Clapp, "A Tutorial on Particle Filters for Online Nonlinear/Non-Gaussian Bayesian Tracking," *IEEE Transactions on Signal Processing*, vol. 50, no. 2, pp. 174–188, 2002.

Copyright © 2025 Advanced Maui Optical and Space Surveillance Technologies Conference (AMOS) – www.amostech.com

[38] J. Kennedy and R. Eberhart, "Particle Swarm Optimization," in *Proceedings of ICNN'95 - International Conference on Neural Networks*, vol. 4, pp. 1942–1948, 1995.

[39] Y. Shi and R. Eberhart, "A Modified Particle Swarm Optimizer," in *1998 IEEE International Conference on Evolutionary Computation Proceedings*, IEEE World Congress on Computational Intelligence, Cat. No. 98TH8360, pp. 69–73, 1998

[40] Q. Qiao, Y. Ping, J. Chen, Y. Lu, and C. Zhang, "Investigation of Factors Affecting the Reflectance Spectra of GEO Satellites," *Advances in Space Research*, vol. 74, no. 7, pp. 3028–3044, 2024.

[41] D. Hall, "Surface Material Characterization from Multi-Band Optical Observations," in *Advanced Maui Optical and Space Surveillance Technologies Conference*, Sept. 2010.

[42] Y. Cao, Z. Wu, L. Bai, and H. Zhang, " Measurement of optical characteristics of solar panels used on satellite," in *Proceedings of the 9th International Symposium on Antennas, Propagation and EM Theory*, IEEE, pp. 746–748, 2010.

[43] K. Levenberg, "A method for the solution of certain non-linear problems in least squares," *Quarterly of Applied Mathematics*, vol. 2, no. 2, pp. 164–168, 1944.

[44] D. W. Marquardt, "An Algorithm for Least-Squares Estimation of Nonlinear Parameters," *Journal of the Society for Industrial and Applied Mathematics*, vol. 11, no. 2, pp. 431–441, 1963.

[45] Hipparchus, "Class LevenbergMarquardtOptimizer," https://www.hipparchus.org/apidocs/org/hipparchus/optim/nonlinear/vector/leastsquares/LevenbergMarquardtOptimizer.html, accessed June 10, 2025.

Copyright © 2025 Advanced Maui Optical and Space Surveillance Technologies Conference (AMOS) – www.amostech.com